International Journal of Heat and Mass Transfer 52 (2009) 5447–5450

Contents lists available at ScienceDirect

International Journal of Heat and Mass Transfer

journal homepage: www.elsevier.com/locate/ijhmt

Convection heat and mass transfer along a vertical heated plate with film evaporation in a non-Darcian porous medium

Jin-Sheng Leu [a,*], Jiin-Yuh Jang [b], Wen-Cheng Chou [b]

[a] Department of Aircraft Engineering, Air Force Institute of Technology, Kaohsiung County 82042, Taiwan
[b] Department of Mechanical Engineering,, National Cheng-Kung University, Tainan 70101, Taiwan

ARTICLE INFO

Article history:
Received 21 October 2008
Received in revised form 25 June 2009
Accepted 26 June 2009
Available online 10 August 2009

Keywords:
Liquid film evaporation
Porous medium
Forced convection

ABSTRACT

A numerical analysis has been carried about to study the heat and mass transfer of forced convection flow with liquid film evaporation in a saturated non-Darcian porous medium. Parametric analyses were conducted concerning the effects of the porosity ε, inlet liquid Reynolds number Re_l, inlet air Reynolds number Re_a on the heat and mass transfer performance. The results conclude that better heat and mass transfer performances are noticed for the system having a higher Re_a, a lower Re_l, and a higher ε. Re_l plays a more important role on the heat and mass transfer performance than Re_a and ε. For the case of $\varepsilon = 0.4$ and $Re_a = 10{,}000$, the increases of Nu and Sh for $Re_l = 50$ are about by 33.9% and 35.3% relative to the values for $Re_l = 250$.

1. Introduction

Fluid flow and heat transfer through saturated porous media has gained much attention because of its wide range of applications in environmental geophysical and energy related engineering problems. An intensive research effort has been devoted in the last decade to problems of natural and mixed convection boundary layer flow along a plate embedded in fluid-saturated porous media. Liquid film evaporation is a gas–liquid flow system with coupled heat and mass transfer at the gas–liquid interface. Because of possessing the advantages of a high heat transfer coefficient, low feed rates, and maintaining the surface at a low temperature, liquid film evaporation problems have received considerable attention and numerous numerical and experimental works have been published. Chun and Seban [1] experimentally observed the evaporation of water from the surface of a falling film flowing turbulently downward on a heated vertical tube and indicated that the Waber number plays an important role in transition. Zheng and Worek [2] measured the local heat and mass coefficients from the air–liquid interface of a falling film by use of a fiber-optic holographic interferometer. The theoretical literature usually analyzed the problem based on the simplified 1-D and 2-D mathematical models (Wassel and Mills [3], Yan and Soong [4], and Tsay [5]). The complete two-dimensional boundary layer model for the evaporating liquid and gas flows was studied by Mezaache and Daguenet [6]. Their parametric study was focused on the effects of inlet conditions such as gas velocity, liquid mass flow rate and inclined angles, and their interaction for both isothermal and heated walls.

In comparison liquid film evaporation in viscous fluid, the applications on the heat and mass transfer of liquid film evaporation in presence of porous medium have attracted less attention. Zhao [7] studied the coupled heat and mass transfer in a stagnation point flow of air through a heated porous bed with thin liquid film evaporation. The numerical solutions are achieved through the simplified assumptions that the liquid layer is very thin and stationary, and the air stream is idealized as the stagnation point flow pattern. Yiotis et al. [8] present a pore-network model to study the drying process in porous media with coupled external and internal mass transfer. Shih et al. [9] studied a steady 2-D laminar mixed convection flow over a vertical wetted plate in a porous medium. The liquid film is assumed to be extremely thin and can be neglected. Thus, the liquid film is reduced to a boundary condition of constant blowing mass flux. Leu et al. [10] evaluated the heat and mass enhancement of liquid film evaporation on the vertical plate with a thin porous layer. The results show that both the Nusselt and Sherwood numbers increase with the decrease of porosity and porous layer thickness.

The present study analyzes the forced convection liquid film evaporation problem in a saturated non-Darcian porous medium. The coupled conservation equations for both the moist-air and liquid film streams are solved together. A non-Darcian model including inertia, boundary and convective effects is employed to represent the momentum transport of these two streams. The parametric studies on the effects of the inlet conditions (inlet air velocity and inlet liquid mass flow rate) and the porosity of the porous medium on the heat and mass performances of liquid film evaporation are examined in detail.

* Corresponding author. Tel.: +886 7 6254168; fax: +886 6 2907047.
E-mail address: willislu@ms13.hinet.net (J.-S. Leu).

0017-9310/$ - see front matter © 2009 Elsevier Ltd. All rights reserved.
doi:10.1016/j.ijheatmasstransfer.2009.06.033

2. Mathematical analysis

Consider a steady two-dimensional laminar forced convection flow over a vertical isothermal heated plate embedded in a porous medium, as shown schematically in Fig. 1. The wall temperature of the plate is T_w. It is wetted by a falling liquid film with an inlet temperature $T_{l,in}$ and inlet flow rate $m_{l,in}$. To facilitate the present study, the following assumptions are prescribed: (1) the air and liquid film are available with the laminar boundary layer assumption. (2) The inlet liquid flow rate is enough small that the surface of the film can be regard as smooth. (3) The porous medium is isotropic and homogeneous, and the convective fluids and the porous matrix are in local thermal equilibrium. (4) The non-Darcian model includes the boundary, inertia, and convective effects. Thermal dispersion and variable porosity effects are neglected. (5) In contrast to the diffusion term, the convective terms in the liquid film momentum equation are neglected.

With the above assumptions and the following dimensionless variables:

$$X=\frac{x}{L},\quad Y_a=\frac{y}{L}\sqrt{\mathrm{Re}_a},\quad Y_l=\frac{y}{\delta(x)},\quad \delta^*=\frac{\delta(x)}{L}$$
$$U_a=\frac{u_a}{u_{a,\infty}},\quad V_a=\frac{v_a}{u_{a,\infty}},\quad U_l=\frac{u_l}{u_{a,\infty}},\quad V_l=\frac{v_l}{u_{a,\infty}}$$
$$\theta_a=\frac{T_a-T_{a,\infty}}{T_w-T_{a,\infty}},\quad \theta_l=\frac{T_l-T_{a,\infty}}{T_w-T_{a,\infty}},\quad \lambda_a=\frac{\omega-\omega_\infty}{\omega_w-\omega_\infty}, \tag{1}$$

The two-dimensional boundary layer equations and boundary conditions of the laminar liquid film flow and air are obtained as follows:

(a) Liquid film region

$$\frac{\partial U_l}{\partial X}+\frac{1}{\delta^*}\frac{\partial V_l}{\partial Y_l}=0 \tag{2}$$
$$0=-\frac{\delta^{*2}}{\mathrm{Da}}U_l-\Gamma\delta^{*2}\nu^*\mathrm{Re}_a U_l^2+\frac{1}{\varepsilon}\frac{\partial^2 U_l}{\partial Y_l^2} \tag{3}$$
$$U_l\frac{\partial\theta_l}{\partial X}+\frac{1}{\delta^*}V_l\frac{\partial\theta_l}{\partial Y_l}=\frac{\nu^*}{\delta^{*2}\mathrm{Pr}_l\mathrm{Re}_a}\frac{\partial^2\theta_l}{\partial Y_l^2} \tag{4}$$

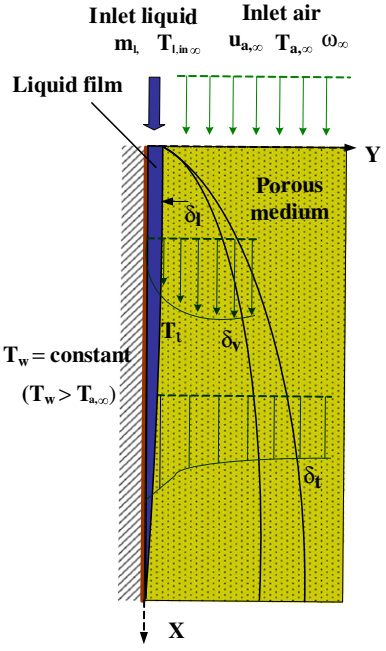

Fig. 1. Schematic diagram of the physical system.

(b) Air stream region

$$\frac{\partial U_a}{\partial X}+\sqrt{\mathrm{Re}_a}\frac{\partial V_a}{\partial Y_a}=0 \tag{5}$$
$$\frac{1}{\varepsilon^2}\left(U_a\frac{\partial U_a}{\partial X}+\sqrt{\mathrm{Re}_a}V_a\frac{\partial U_a}{\partial Y_a}\right)=\frac{1}{\mathrm{DaRe}_a}(1-U_a)+\Gamma(1-U_a^2)+\frac{1}{\varepsilon}\frac{\partial^2 U_a}{\partial Y_a^2} \tag{6}$$
$$U_a\frac{\partial\theta_a}{\partial X}+\sqrt{\mathrm{Re}_a}V_a\frac{\partial\theta_a}{\partial Y_a}=\frac{1}{\mathrm{Pr}_a}\frac{\partial^2\theta_a}{\partial Y_a^2} \tag{7}$$
$$U_a\frac{\partial\lambda_a}{\partial X}+\sqrt{\mathrm{Re}_a}V_a\frac{\partial\lambda_a}{\partial Y_a}=\frac{1}{\mathrm{Pr}_a\mathrm{Le}}\frac{\partial^2\lambda_a}{\partial Y_a^2} \tag{8}$$

(c) The dimensionless boundary conditions

$$\text{at inlet } (X=0)\qquad \theta_l=\theta_{l,in},\quad \theta_a=0,\quad U_a=1,\quad \lambda_a=0 \tag{9}$$

at wall and outside border ($Y_l = 0$, $Y_a = \infty$)

$$\text{at } Y_l=0,\qquad U_l=0,\quad V_l=0,\quad \theta_l=1 \tag{10}$$
$$\text{at } Y_a=\infty,\qquad U_a=1,\quad V_a=0,\quad \theta_a=0,\quad \lambda_a=0$$

at air–liquid interface ($Y_l = 1$)

$$U_i=U_{l,i}=U_{a,i},\quad \theta_i=\theta_{l,i}=\theta_{a,i} \tag{11}$$
$$V_{a,i}=-\frac{(\omega_w-\omega_\infty)}{(1-\omega_i)}\frac{1}{\mathrm{Pr}_a\mathrm{Le}\sqrt{\mathrm{Re}_a}}\left(\frac{\partial\lambda_a}{\partial Y_a}\right)_i \tag{12}$$
$$\left(\frac{\partial U_l}{\partial Y_l}\right)_i=\sqrt{\mathrm{Re}_a}\left(\frac{\rho_a}{\rho_l}\right)\frac{\delta^*}{\nu^*}\left(\frac{\partial U_a}{\partial Y_a}\right)_i \tag{13}$$
$$\left(\frac{\partial\theta_l}{\partial Y_l}\right)_i=\sqrt{\mathrm{Re}_a}\frac{k_a}{k_l}\delta^*\left(\frac{\partial\theta_a}{\partial\eta_a}\right)_i+\sqrt{\mathrm{Re}_a}\frac{\rho_a D h_{fg}\delta^*(\omega_w-\omega_\infty)}{k_l(T_w-T_\infty)(1-\omega_i)}\left(\frac{\partial\lambda_a}{\partial Y_a}\right)_i \tag{14}$$

where ρ, k, ν, α, and D are the effective density, thermal conductivity, kinematic viscosity, thermal diffusivity and mass diffusivity. δ^* is the ratio of liquid film thickness to plate length, ω_w is the corresponding mass concentration at the wall temperature T_w. h_{fg} is the latent heat of vaporization. The subscript "l" and "a" represent the variables of the liquid and air streams.

The dimensionless parameters in Eqs. (2)–(14) are defined as follows: $\nu^* = \nu_l/\nu_a$ is the kinematic viscosity ratio of liquid to air, $\mathrm{Da} = K/L^2$ is the Darcy number of porous medium, $\Gamma = CL$ is the dimensionless inertia coefficient, $\mathrm{Re} = uL/\nu$ is the Reynolds number, $\mathrm{Pr} = \nu/\alpha$ is the Prandtl number, and $\mathrm{Le} = \alpha/D$ is the Lewis number. The parameters K and C are the permeability and inertia coefficients of the porous medium, which can be determined from the correlations $K = d_p^2\varepsilon^3/[150(1-\varepsilon)^2]$, $C = 1.75(1-\varepsilon)/(d_p\varepsilon^3)$ (proposed by Ergun [11], d_p is the particle diameter of porous medium).

The dimensionless equation of conservation of liquid mass flow rate at each location along the plate can be expressed as:

$$1=\frac{(\mathrm{Re}_a\rho_a)/(\rho_l\nu^*)}{(\mathrm{Re}_l/4)}\int_0^X V_a dX+\frac{\mathrm{Re}_a\delta^*/\nu^*}{(\mathrm{Re}_l/4)}\int_0^1 U_l dY_l \tag{15}$$

where $\mathrm{Re}_l = 4m_{l,in}/\mu_l$ is the inlet liquid Reynolds number. The local heat transfer coefficient $h_{t,x}$ and local mass transfer coefficient $h_{m,x}$ at the interface are defined as:

$$h_{t,x}=\frac{q_t''}{(T_w-T_{a,\infty})}=\frac{\left(-k_a\frac{\partial T}{\partial y}\right)_i}{(T_w-T_{a,\infty})}+\frac{m_v''\cdot h_{fg}}{(T_w-T_{a,\infty})} \tag{16}$$
$$h_{m,x}=\frac{m_{v,i}''(1-\omega_i)}{\rho_a(\omega_w-\omega_\infty)} \tag{17}$$

It should be noted that the reference temperature difference used in Eq. (17) is defined as $(T_w - T_{a,\infty})$ instead of $(T_i - T_{a,\infty})$. This is because $(T_i - T_{a,\infty})$ is an unknown and changeable value, and is not applicable for non-dimensionalized analysis. The average Nusselt and Sherwood numbers over the length (L) of the plate are written as

$$\mathrm{Nu} = \frac{\int_0^L h_{t,x}dx}{k_a}, \quad \mathrm{Sh} = \frac{\int_0^L h_{m,x}dx}{D} \tag{18}$$

3. Numerical method

The coupled governing equations (2)–(8) are parabolic at X, and thus the finite difference solutions for these equations can be marched along the downstream direction at the beginning with $X = 0$. The governing equations are discretized to a fully implicit difference representation, in which the upwind scheme is used to model the axial convective terms, while second-order central difference schemes are employed for the transverse convection and diffusion terms. The Newton linearization procedure is used to linearize the nonlinear terms of Eqs. (2)–(8). In what follows, the discretization equations can be written in "block-tri-diagonal" form and solved by the tri-diagonal matrix method. The detail of numerical procedure is described in Leu et al. [10].

4. Results and discussion

The present study mainly describes the local and overall heat and mass transfer characteristics of forced convection liquid film evaporation flow in a saturated porous medium. The parametric analysis is focused on the coupled effects of the porosity ε and inlet liquid Reynolds number $\mathrm{Re_l}$ on the heat and mass transport phenomena. With regard to practical situations, certain conditions are assigned: $P_\infty = 1$ atm, $T_w = 60$ °C, $T_{l,in} = T_{a,\infty} = 27$ °C, $\phi = 70\%$, and $L = 0.5$ m. The liquid in the present study is supposed to be water.

Fig. 2 presents the axial distributions of dimensionless liquid–air interfacial temperature θ_i for various inlet liquid Reynolds number $\mathrm{Re_l}$ and porosity ε at $\mathrm{Re_a} = 10{,}000$. As shown in Fig. 2, θ_i initially dramatically increases with the axial location X, and finally reaches an asymptotic maximum. The cases of lower inlet liquid Reynolds number ($\mathrm{Re_l} = 50$) are especially significant. This is because a lower inlet liquid mass flow rate induces a thinner liquid film, which is easier to be heated and then produces a higher interfacial temperature. Fig. 2 also shows that higher θ_i is found for the cases of higher ε. The reason is the flow in a highly porous medium has a more violent velocity field and higher heat transfer performance. It is noted that the results for $\varepsilon = 1$ correspond to the case of liquid film evaporation flow without porous medium [6]. Meanwhile, a large amount of evaporating flux of liquid film happens at the front region of the heated plate (within the region of $0 < X < 0.4$). The reason is the front region has higher temperature and mass concentration gradients between the liquid–air interface and air flow. The extended result concludes that the consumption of the liquid water is increased with $\mathrm{Re_a}$ and larger consumption ratio of liquid water is observed in the cases of lower $\mathrm{Re_l}$. For the present study, the mass lose of liquid film due to evaporation is relatively small and at most 6% of inlet liquid mass flow rate.

The coupled effects of $\mathrm{Re_l}$ and ε on the average Nusselt number (Nu) and average Sherwood number (Sh) are indicated in Fig. 3, which shows the variations of Nu and Sh versus $\mathrm{Re_l}$ for various porosity ε and particle diameter d_p at $\mathrm{Re_a} = 10{,}000$. It shows that larger values of Nu and Sh appear in the cases with the trends of lower $\mathrm{Re_l}$, higher ε and higher d_p. And the values of Nu and Sh decrease with the increase in $\mathrm{Re_l}$, especially for low-porosity porous medium ($\varepsilon = 0.4$). For the case of $\varepsilon = 0.4$ and $d_p = 3$ mm, the values of Nu and Sh at $\mathrm{Re_l} = 250$ are reduced by 25.3% and 26.1% relative to the values at $\mathrm{Re_l} = 50$, respectively. Meanwhile, the effect of porosity ε on the Nu and Sh are gradually apparent while the $\mathrm{Re_l}$ increases. For $\mathrm{Re_l} = 50$ and $d_p = 3$ mm, the increases of Nu and Sh at $\varepsilon = 0.7$ are about 1.9% and 2.2% to these values at $\varepsilon = 0.4$. The corresponding increases for $\mathrm{Re_l} = 250$ are about 11.3% and 13.2%. Thus, the conclusion can be drawn that $\mathrm{Re_l}$ plays a more important role than porosity ε and particle diameter d_p on the heat and mass transfer performances of this problem.

5. Conclusions

The characteristics of liquid film evaporation in forced convection flow in a porous medium were studied. The complete two-dimensional laminar boundary layer models for the evaporating liquid and air flows along a vertical plate were adopted. The non-Darcian convective, boundary viscous, and inertia force effects are considered. From the present results, the following conclusions are achieved:

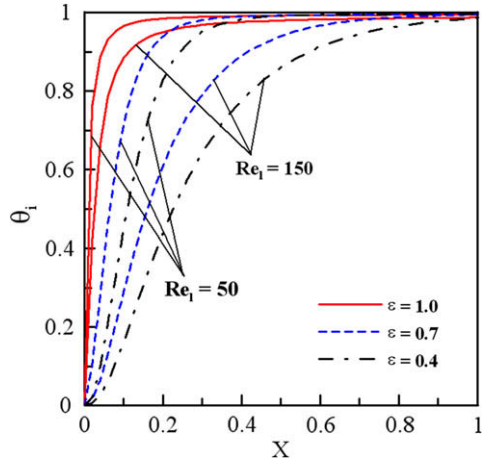

Fig. 2. The developments of dimensionless interfacial temperature θ_i along the liquid–air interface for various $\mathrm{Re_l}$ and porosity ε at $\mathrm{Re_a} = 10{,}000$.

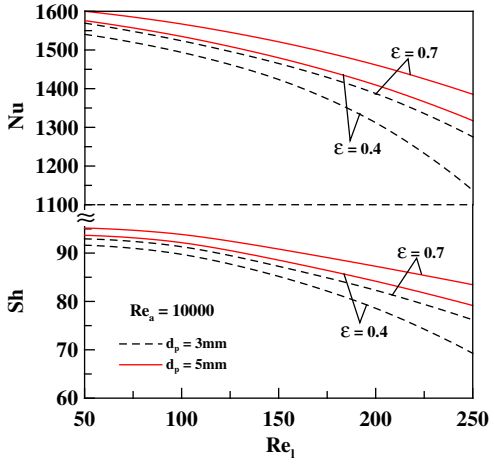

Fig. 3. The coupled effects of the $\mathrm{Re_l}$, ε, and d_p on the average Nusselt number and Sherwood number at $\mathrm{Re_a} = 10{,}000$.

(1) The latent heat transfer is still the dominant mode for the present study. The mass transfer flux concentrates in the entrance region of the plate.
(2) The cases of lower Re_l and larger ε have larger consumption ratio of liquid water. The mass lose of liquid film due to evaporation is small and liquid consumption ratio is within 6%.
(3) Lower Re_l and higher ε make liquid film higher interfacial temperature and mass concentration, thus enhance the heat and mass transfer performances across the film interface. For $\varepsilon = 0.4$ and $d_p = 3$ mm, the increases of Nu and Sh at $Re_l = 50$ are about by 33.9% and 35.3% relative to the values at $Re_l = 250$, respectively.
(4) The influences of Re_l on the heat and mass transfer performance of liquid film evaporation in porous medium are more important than the influences of ε and d_p.

Acknowledgement

The authors are grateful to the National Science Council of Taiwan for financial support in this work, under Contract NSC 95-2221-E-344-003.

References

[1] K.R. Chun, R.A. Seban, Heat transfer to evaporating liquid films, J. Heat Transfer ASME 93 (1971) 391–396.
[2] G.S. Zheng, W.M. Worek, Method of heat and mass transfer enhancement in film evaporation, Int. J. Heat Mass Transfer 39 (1996) 97–108.
[3] A.T. Wassel, A.F. Mills, Design methodology for a counter-current falling film evaporative condenser, ASME J. Heat Transfer 109 (1987) 784–787.
[4] W.M. Yan, C.Y. Soong, Convection heat and mass transfer along an inclined heated plate with film evaporation, Int. J. Heat Mass Transfer 38 (1995) 1261–1269.
[5] Y.L. Tsay, Heat transfer enhancement through liquid film evaporation into countercurrent moist air flow in a vertical plate channel, Heat Mass Transfer 30 (1995) 473–480.
[6] E. Mezaache, M. Daguenet, Effects of inlet conditions on film evaporation along an inclined plate, Solar Energy 78 (2005) 535–542.
[7] T.S. Zhao, Coupled heat and mass transfer of a stagnation point flow in a heated porous bed with liquid film evaporation, Int. J. Heat Mass Transfer 42 (1999) 861–872.
[8] A.G. Yiotis, I.N. Tsimpanogiannis, A.K. Stubos, Y.C. Yortsos, Coupling between external and internal mass transfer during drying of a porous medium, Water Resour. Res. 43 (2007) W06404.
[9] M.H. Shin, M.J. Huang, C.K. Chen, A study of the liquid evaporation with Darcian resistance effect on mixed convection in porous media, Int. Commun. Heat Mass Transfer 32 (2005) 685–694.
[10] J.S. Leu, J.Y. Jang, Y. Chou, Heat and mass transfer for liquid film evaporation along a vertical plate covered with a thin porous layer, Int. J. Heat Mass Transfer 49 (2006) 1937–1945.
[11] S. Ergun, Fluid flow through packed columns, Chem. Eng. Prog. 48 (1952) 89–94.